Journal of Inorganic and Organometallic Polymers and Materials (2018) 28:805–811
https://doi.org/10.1007/s10904-017-0747-x

A Novel In-Situ Synthesis and Enhanced Photocatalytic Performance of Z-Scheme Ag/AgI/AgBr/Sulfonated Polystyrene Heterostructure Photocatalyst

Bing Song[1] · Qingjie Tang[1] · Wenrong Wu[1] · Huoli Zhang[1] · Jianliang Cao[1] · Mingjie Ma[1]

Received: 21 September 2017 / Accepted: 19 November 2017 / Published online: 24 November 2017

Abstract
Novel Z-scheme Ag/AgI/AgBr/sulfonated polystyrene composite is prepared via ion-exchange followed by light reduction. The photocatalytic activities of as-synthesized samples are evaluated through the degradation of methyl orange (RhB) under visible light irradiation. The Z-scheme Ag/AgI/AgBr/SPs photocatalysts display excellent photocatalytic activity and stability compared with Ag/AgI and Ag/AgBr. The improved photocatalytic activity is mainly due to the combined effects of the Z-scheme structure of Ag/AgI/AgBr/SPs and the strong surface plasmon resonance effect of Ag^0 nanoparticles. Moreover, after four successive cycles, the Ag/AgI/AgBr/SPs photocatalysts have no obvious loss of activity for the degradation of RhB, illustrating that the Z-scheme Ag/AgI/AgBr/SPs photocatalysts are rather stable under visible-light irradiation.

Keywords Ag/AgI/AgBr · Polymers · Optical materials and properties · Semiconductors

1 Introduction

It is well known that environmental pollution has become a serious problem around the world. Especially, the modern society and industry have made great development in the present century. To solve the trouble, in the past few decades, many semiconductor photocatalysts have been exploited and used for the researches about pollution management of water environment and solar energy conversion. Among numerous photocatalysts, TiO_2 has become the most widely investigated and used photocatalyst due to its excellent performance such as low cost, non-poisonous and high resistance against chemical and light corrosion. However, the large band gap tremendously limits the practical application of titanium dioxide, because only a small scale of ultraviolet light in the sun light can stimulate TiO_2 for photocatalytic reaction. Therefore, it is a research focus to find and develop novel photocatalytic materials with low band gap and strong absorption property to visible light.

In recent years, Ag-based functional materials have aroused great concern due to the enhanced absorption in the visible light region and the improved photocatalytic activity [1–8]. Moreover, there is a similar photoexcitation process for pure silver halides (AgX, X = Cl, Br and I). By absorbing incident light, the photogenerated electrons and holes produce from the conduction band (CB) and valence band (VB), respectively. The electrons in the CB can be captured by surface lattice Ag^+ ions to form metallic Ag^0, While the photogenerated holes have strong oxidation performance and oxidize lattice X^- to release X_2, resulting in the photodecomposition of silver halides. Considering the fact that the Z-scheme heterostructure [9–17] is beneficial to enhance the transfer rate of photogenerated electrons to improve the photoinduced stability. In this paper, we design a novel Z-scheme Ag/AgI/AgBr/sulfonated polystyrene heterostructure photocatalyst. Due to the photogenerated holes in the AgBr has a higher VB maximum and the photogenerated electrons in the AgI possesses a lower CB minimum, promoted by the electron mediator. It is quite possible to construct a high efficiency Z-scheme photocatalyst and thus improving the photocatalytic activity and stability.

Sulfonated polystyrene (SPs) is a polymer compound with ion exchange function, and it has been applied to various of exchange processes [18–20] due to its big specific surface area, faster rate of exchange and elution, high regeneration

✉ Qingjie Tang
tangqj521@163.com

[1] College of Chemistry and Chemical Engineering, Henan Polytechnic University, Jiaozuo 454000, Henan, China

performance, low consumption and small fluid resistance. Thousands of factories have been built in recent years and a great amount of organic pollutants and heavy metal ions were discharged into rivers. Compared with the traditional handing methods, ion exchange from sulfonated polystyrene possesses high efficiency, convenient, non-poisonous and lower cost, etc. Considering the fact that photocatalysts power is easily agglomerated in aqueous solution and the photocatalytic activity is affected by a certain degree. We decide to utilize sulfonated polystyrene as carrier to combine with the metal ions in aqueous solution through ion exchange reaction and then add some anion for synthesizing photocatalysts. Due to the distribution of ion exchange sites on the sulfonated polystyrene are very uniform, therefore, the metal semiconductors will also be evenly distributed on the resin surface. This can efficiently suppress the agglomeration of photocatalyst power and increase the contact areas between photocatalyst and organic pollutants in the photodegradation so as to improve the photocatalytic activity.

Here, we decided to utilize sulfonated polystyrene to recycle silver ion from simulated wastewater containing silver ion ($AgNO_3$ aqueous solution) to prepare Ag/AgI/AgBr/sulfonated polystyrene (Ag/AgI/AgBr/SPs) photocatalyst with heterojunction structure via in-situ ion exchange followed by light reduction method. This will not only provide a practical method for solving the problem of silver ion recycling, we can also obtain a high efficiency photocatalytic material, it can be described as two birds with one stone. What's more, the as-prepared photocatalyst exhibits superior photocatalytic properties and stability compared with Ag/AgBr and Ag/AgI. The enhancement is mainly attributed to the heterojunction structure. The possible mechanism for the photodegradation of Ag/AgI/AgBr/SPs was also tentatively proposed.

2 Experimental

2.1 Materials and Reagents

The reagent styrene (98%) and polyvinylpyrrolidone (PVP) used as stabilizer purchased from was purchased from Aladdin (China). 2, 2′-Azobis (2-methylpropionitrile) (AIBN, 98%) used as initiator was purchased from Shanghai Macklin Biochemical Co., Ltd. $AgNO_3$, KBr, KI, NaOH and all other reagents were analytical grade without further purification and purchased from Luoyang chemical reagent factory.

2.2 Synthesis of Sulfonated Polystyrene Microsphere

The sulfonated polystyrene microsphere used as template was synthesized by dispersion polymerization. 10 g styrene, 0.5 g PVP, 0.3 g AIBN and 120 mL ethanol were added to three-necked flask and the mixture was mechanical stirred at 70 °C for 12 h. The product was centrifuged and washed with deionized water and ethanol for several times, and then dried at 60 °C for 12 h. 3 g as-prepared polystyrene microsphere and 90 mL sulfuric acid were added into flask and the mixture was mechanical stirred at 50 °C for 12 h. The obtained sulfonated polystyrene microsphere was centrifuged and washed with deionized water until the pH was 7 and then dried at 60 °C for 12 h.

2.3 Synthesis of Ag/AgI/AgBr/SPs

A certain amount of as-prepared sulfonated polystyrene microspheres (the specific dosage is found in Chap. 3.1) were added to 100 mL aqueous solution containing $AgNO_3$ (0.169 g) and stirred for 8 h at room temperature. Then 100 mL of 0.01 M KBr aqueous solution was poured into the solution and continuous stirring. After 5 min, the faint yellow product was separated by centrifugation and washed with deionized water for several times, redispersed in 100 mL of deionized water. Then KI aqueous solution was added in the above suspension and continuous stirring for 1 h, after that it was irradiated with a 500 W Xe lamp for 30 s to form a certain amount of Ag^0 NPs on the surface of product. Finally, the obtained Ag/AgI/AgBr/SPs was centrifuged, washed, dried.

2.4 Characterization

The X-ray diffraction (XRD) pattern of the as-prepared Ag/AgI/AgBr/SPs microspheres were obtained on a Bruker D8 Advance X-diffractometer (Cu Kα radiation, 2θ range 20°–80°). Chemical components and valence states were recorded on X-ray photoelectron spectroscopy (Thermo escalab 250Xi). The surface morphology of sample was investigated by a field emission scanning electron microscope (S-4800 FESEM; Hitachi). Optical absorption spectra was analyzed by a Pgeneral TU-1901 UV–Vis spectrophotometer equipped with an integrating sphere assembly.

2.5 Photocatalytic Degradation of Pollutants Under Visible Light Irradiation

The studies of photocatalytic activity were proceeded under a 500 W Xe lamp with a UV-cutoff filter ($\lambda > 425$ nm) and Rhodamine B (RhB) was used as the target organic pollution. The samples (50 mg) were put into 100 mL of RhB aqueous solution (15 mg/L). The suspensions were kept in the dark for 30 min with magnetically stirring to establish an adsorption–desorption equilibrium. At a given time interval, 10 mL of solution was collected and centrifuged. Then

concentrations of the centrifuged solution were detected with a DR2800-water quality analyzer (HACH, America).

3 Results and Discussion

3.1 Effect of Resin Dose on the Removal Rate of Silver Ion in the Aqueous Solution

A certain amount of as prepared sulfonated polystyrene microspheres (0.4, 0.6, 0.8, 1.0, 1.2 g) was added into conical flask, respectively. Then 100 mL simulated wastewater containing silver ion (0.01 mol/L $AgNO_3$ aqueous solution) was added in each flask. All flasks were put in water-bathing constant temperature vibrator and oscillated at room temperature for 2 h. When it is over, flasks were taken out and Ag^+ concentration of aqueous solution was determined by atomic absorption spectrometry, finally, we could work out the removal rate of Ag^+ according to the following the formula:

$$E\% = \left(C_0 - C\right)/C_0 \times 100\%$$

wherein E% represents the removal rate of Ag^+, C_0 stands for the initial concentration of Ag^+, C represents the residual concentration of Ag^+ in aqueous solution.

Figure 1 displays the effect of resin dose on the removal rate of silver ion. As seen, before the dose reached 1.0 g, lots of silver ions in the solution could be combined with the sulfonic acid groups on the surface of resin by ion-exchange reaction and with the increase in the amount of resin, the removal rate of silver ion also enhanced. While the amount more than 1 g, the entire system basically reached saturation, even if we increased the resin, the removal rate was difficult to further promote. Therefore, we decided to use 1.0 g as-prepared sulfonated polystyrene microspheres to synthesize the Ag/AgI/AgBr/sulfonated polystyrene (Ag/AgI/AgBr/SPs) photocatalyst.

3.2 XRD Analysis

Figure 2 illustrates the XRD pattern of the as-prepared samples. Patterns a and c indicate that the characteristic peaks of AgBr and AgI consist with the standard card of JCPDS 06-4308 and JCPDS 09-0374, respectively. When AgI/AgBr heterostructure are formed through the ion exchange process, the XRD patterns of as-prepared samples change correspondingly. As shown in pattern b, some weak peaks at 22.3°, 23.7°, 25.3°, 39.2°, 42.6° and 46.3° appear on AgBr phase and they are ascribed to the (1 0 0), (0 0 2), (1 0 1), (1 1 0), (1 0 3) and (1 1 2) crystal planes of AgI. Additionally, no apparent peaks indexed to metallic Ag are observed owing to its low amount. These observations demonstate the successful grafting of AgI onto AgBr particles.

3.3 Morphology of Ag/AgI/AgBr/SPs Heterostructure Photocatalyst

The SEM images of as-prepared samples are shown in Fig. 3. It can be seen that the as prepared Ag/AgI/AgBr/SPs are of spherical morphology with the diameter of about 1 μm (Fig. 3a–b). What's more, as shown in Fig. 3c–d, the surface of pure SPs is smooth while that of Ag/AgI/AgBr/SPs is rather rough. This mainly due to the fact that AgI and AgBr are in-situ formed on the surface of pure SPs after ion exchange processes, which make the smooth surface of SPs become crude. The EDS indicates that Br, Ag, I elements coexisted in the sample with molar ratio of 40.52:51.56:7.92 and the amount of Ag element is more than the total amount of Br and I, which illuminates that the partial AgI and AgBr have been transformed to Ag^0 NPs through photoreduction.

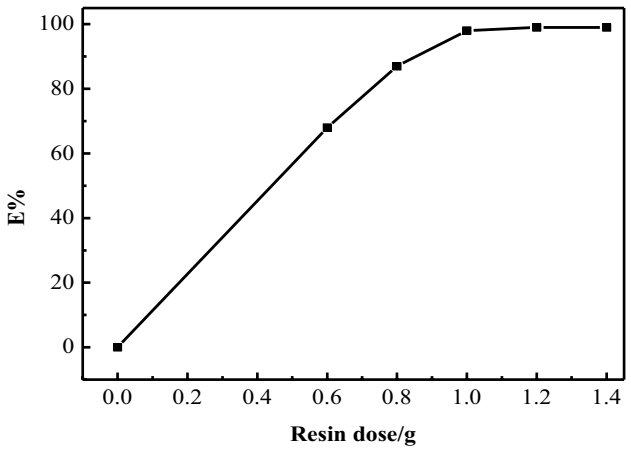

Fig. 1 Effect of resin dose on the removal rate of silver ion

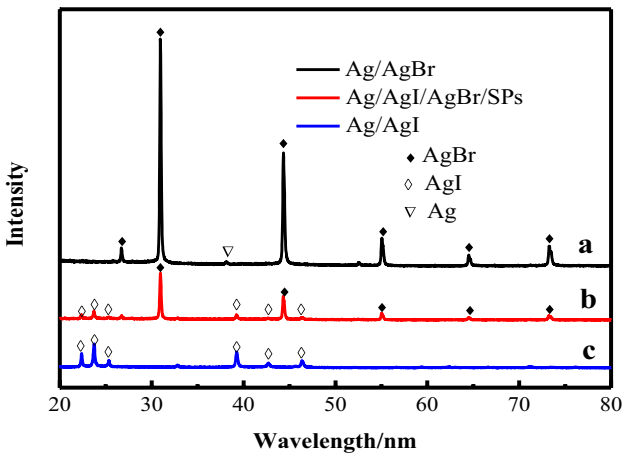

Fig. 2 XRD pattern of the as-synthesized samples

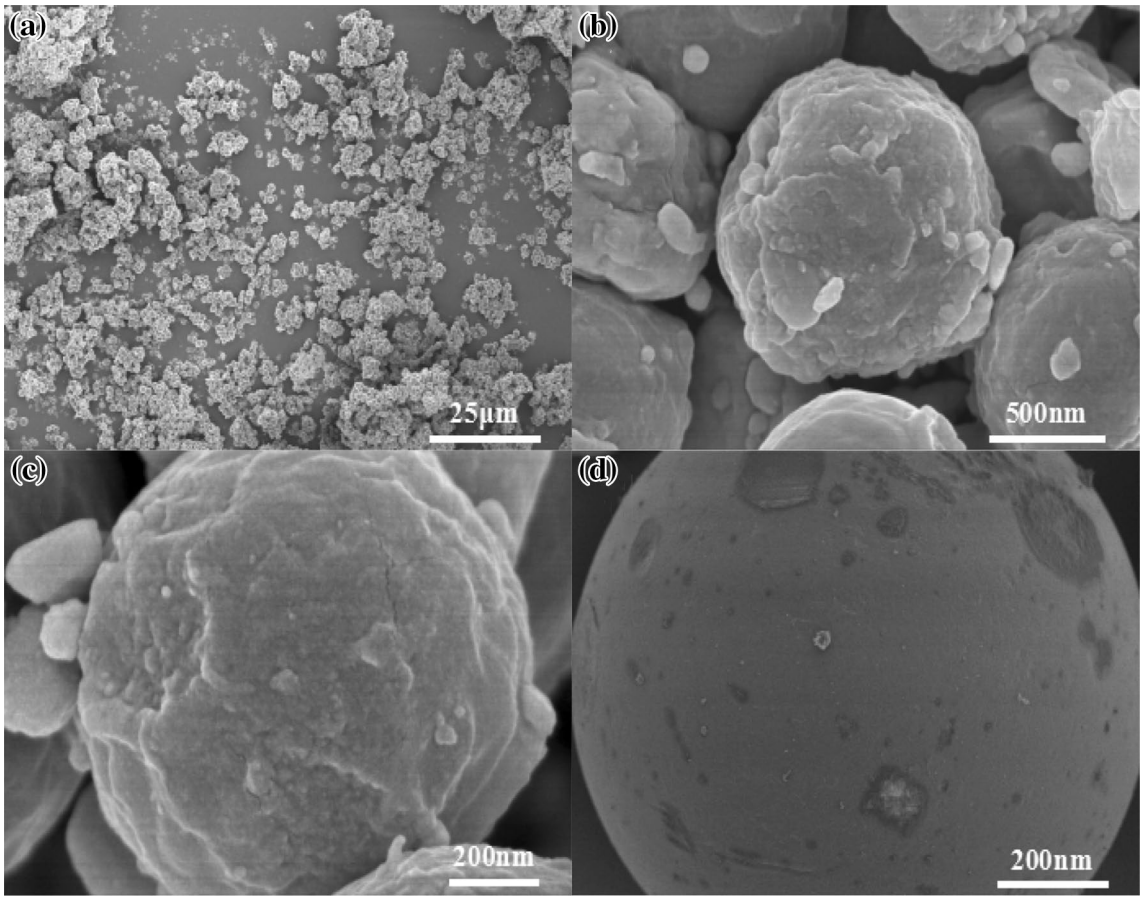

Fig. 3 SEM images of Ag/AgI/AgBr/SPs (**a**–**c**) and SPs (**d**)

3.4 Elemental Chemical Status of the Catalysts

In order to further confirm the chemical state and elemental composition of Ag/AgI/AgBr/SPs heterostructure photocatalyst, XPS of the smples is carried out. Figure 4a displays the whole XPS spectrum of the as-prepared samples, which mainly shows the peaks of Ag, Br, I, C, O. The sources of the peaks are sulfonated polystyrene, $AgNO_3$, KBr, NaI, respectively. Figure 4b shows the Ag 3d spectrum. Peaks at 374 and 368 eV are attributed to Ag $3d_{3/2}$ and Ag $3d_{5/2}$ binding energies, respectively, demonstrating the presence of Ag^+ ions in AgBr and AgI. And no apparent peaks

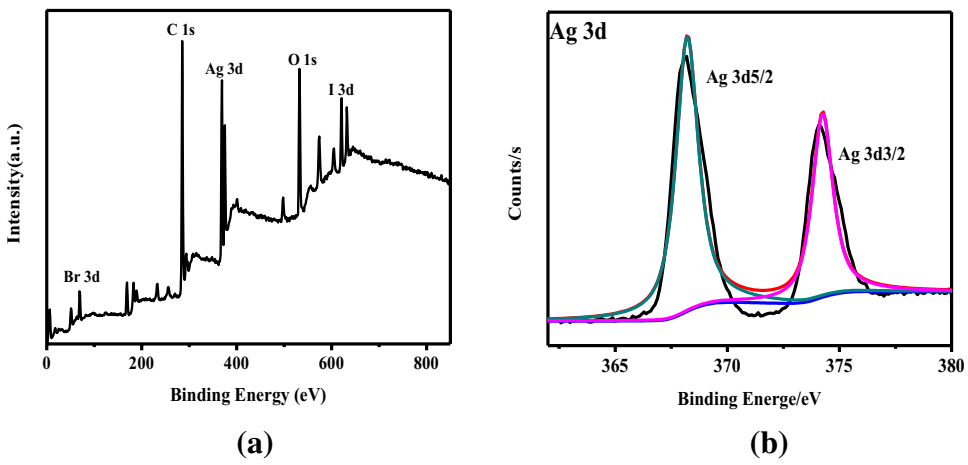

Fig. 4 **a** the whole XPS spectrum of the as-prepared samples, **b** the XPS spectrum of Ag 3d

belonging to the Ag^0 appear, illustrating its low amount. The result reveals the formation of AgI/AgBr heterostructure.

3.5 UV–Vis Diffuse Reflectance Spectra Analysis

The UV–Vis diffuse reflectance spectra of the as prepared AgBr, AgI and Ag/AgI/AgBr/SPs photocatalysts are illustrated in Fig. 5a, respectively. The band gap (E_g) of AgBr and AgI are obtained from a plot of $(\alpha h\nu)^{2/n}$ versus photon energy ($h\nu$) (Fig. 5b). Bare AgI has an absorption edge at the wavelength of about 460 nm corresponding to 2.7 eV of band gap. While pure AgBr nanoparticles display strong absorption in visible light region that should be due to its narrower band gap (2.55 eV). As for Ag/AgI/AgBr/SPs, the sample exhibits a stronger response in the visible light region than pure AgBr and AgI samples. In addition, it also can be observed that there is a shoulder in the wavelength range of 480–800 nm, which can be ascribed to the surface plasmon resonance effect of Ag NPs [21–23].

3.6 The Photocatalytic Activity and Stability

The photocatalytic activity of as-synthesized samples are evaluated by photodegradation of RhB. C/C_0 represents the concentration ratio after and before a certain reaction time. As shown in Fig. 6a, in the absence of photocatalyst, the concentrations of the pure RhB solution are almost unchanged after visible light irradiation for 40 min. However, when the as-prepared Ag/AgBr, Ag/AgI and Ag/AgI/AgBr/SPs photocatalysts are added and they exhibite the different photocatalytic activities for the RhB degradation reaction. After irradiated under visible light for 40 min, the RhB is degraded for 47, 11.1 and 98.6%, respectively. Obviously, the Ag/AgI/AgBr/SPs photocatalyst displays the highest photocatalytic activity. This mainly due to the construction of Z-scheme heterostructure and the SPR effect of Ag NPs.

Figure 6b is the first-order kinetics data of the exponential decay with the time, and the value of the kinetics constant K (K is calculated using the formula of $-\ln(C/C_0) = Kt$, where C is the concentration of the RhB at time t, C_0 is the initial concentration of the RhB solution, t is the reaction time) are shown in Fig. 6c, which indicates that the photocatalytic process follows the pseudo-first-order reaction [24]. As seen, the kinetic constants of Ag/AgI, Ag/AgBr and Ag/AgI/AgBr/SPs for the photodegradation of RhB are 0.003, 0.016 and 0.093 min^{-1}, respectively. The Ag/AgI/AgBr/SPs exhibits the highest degradation rate and its rate constant is about 5.8 and 31 times higher than that of Ag/AgBr and Ag/AgI. The stability of the catalyst is very important for its practical applications. Therefore, the repetition tests of the Ag/AgI/AgBr/SPs microspheres were carried out and the results were shown in Fig. 6d. After four cycles, the degradation yield was slightly reduced, which displayed the excellent stability of the Ag/AgI/AgBr/SPs catalyst.

3.7 Possible Photocatalytic Mechanism

First, under visible light irradiation, a series of reactive species are produced in the photodegradation process of organic pollutants. In order to determine the kind of reactive species in the Ag/AgI/AgBr/SPs photocatalytic system, the quenchers of benzoquinone (BQ), ammonium oxalate (AO) and isopropyl alcohol (IPA) are introduced into the photodegradation process of organic pollutants. In this study, the BQ, AO and IPA are used as superoxide anions ($\cdot O_2^-$), hole (h^+) and hydroxyl radicals (·OH) scavengers, respectively.

Figure 7 shows the results of trapping experiment. It can be clearly seen that the degradation efficiency is almost unchanged in the presence of AO and IPA, However, when the BQ is added, only 52% of RhB is degraded under the same condition, indicating that the superoxide anions ($\cdot O_2^-$) is the main reactive species for the degradation of RhB over the Ag/AgI/AgBr/SPs photocatalyst.

Second, the ability of a semiconductor to transfer photoexcited electrons to species adsorbed on its surface is governed by the band energy position of the semiconductor and the

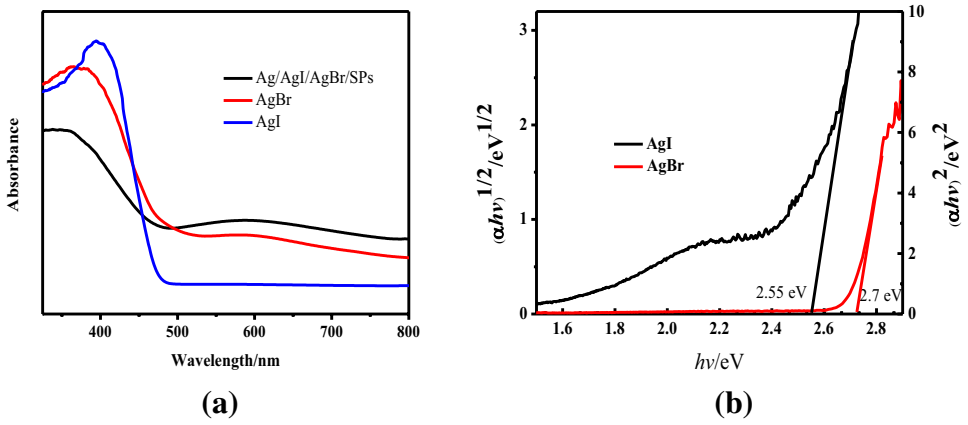

Fig. 5 **a** DRS of the as-prepared photocatalysts, **b** Plot of $(\alpha h\nu)^{1/2}$ versus $h\nu$ for the E_g of AgBr and the plot of $(\alpha h\nu)^2$ versus $h\nu$ for the E_g of AgI

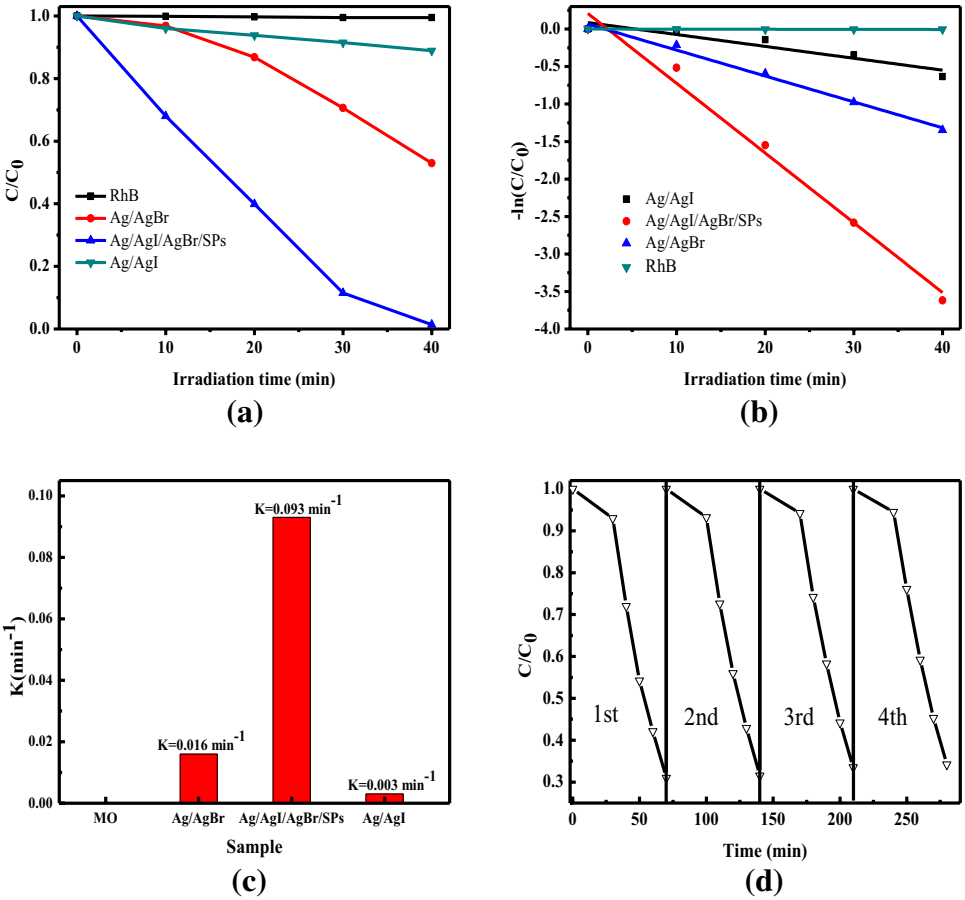

Fig. 6 **a** Photocatalytic activity of as-prepared samples for the degradation of RhB in visible light, **b** kinetics curve, **c** constant K, **d** recycle curve of Ag/AgI/AgBr/SPs

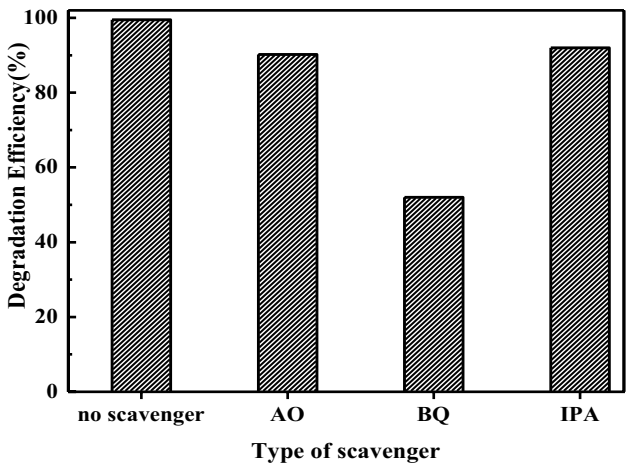

Fig. 7 Photocatalytic activity for degradation of RhB in the presence of different quenchers under light irradiation

redox potentials of the adsorbate [25]. Therefore, the positions of CB and the VB edge are calculated according to the following empirical equations [26]:

$$\chi(S) = \sqrt[N]{\chi_1^{\,n}\chi_2^{\,s}\cdots\chi_{n-1}^{\,p}\chi_n^{\,q}} \quad (1)$$

$$E_{VB} = \chi(S) - E^{e} + 0.5E_g \quad (2)$$

$$E_{CB} = E_{VB} - E_g \quad (3)$$

where χ_n, n, N, E_g and E^e are the electronegativity of the constituent atom, the number of species, the total number of atoms, the band gap energy of the semiconductor and the energy of free electrons on the hydrogen scale (~4.5 eV) in the compound, respectively. The band gap (E_g) of AgBr and AgI are obtained from a plot of $(\alpha h\nu)^{2/n}$ versus photon energy ($h\nu$) and the E_g of AgBr and AgI are estimated to be 2.55 and 2.7 eV, respectively.

Therefore, the E_{VB} of AgBr and AgI are calculated to be 2.595 and 2.33 eV, respectively. And the E_{CB} of them are 0.045 and − 0.37 eV, separately.

Based on the above results, a possible photocatalytic mechanism of the Ag/AgI/AgBr/SPs photocatalysts under visible light irradiation is proposed and illustrated in Fig. 8. Under visible light irradiation. Both AgBr and AgI are excited to produce electrons and holes. Due to the Fermi level of Ag is more positive than the CB potential of AgBr, the photogenerated electrons transfer from the CB of AgBr to Ag^0 [27] and then continued to move to the VB of AgI (2.33 eV), recombing with the holes. Hence, the Z-scheme

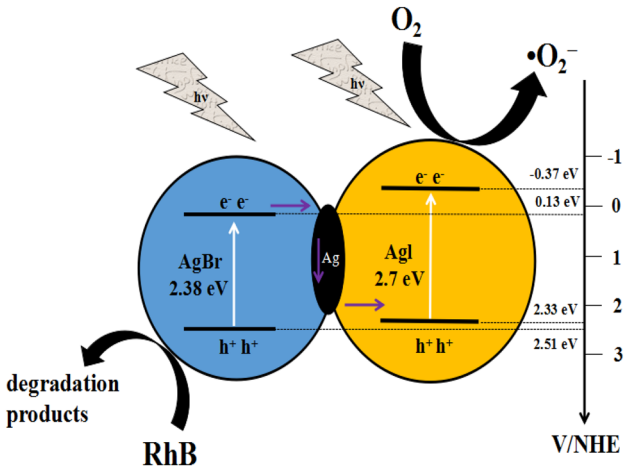

Fig. 8 Possible photocatalytic mechanism of Ag/AgI/AgBr/SPs under visible light

structure is built between AgBr and AgI. Since the VB of AgBr possesses more positive potential and the electrons located on the CB of AgI have strong reduction ability. The photogenerated holes of AgBr valance band (2.595 eV) will degrade the RhB directly and the electrons located on the CB of AgI (−0.37 eV) will be trapped by O_2 to form $\cdot O_2^-$ that further decompose organic pollutants. Some similar mechanism has been studied by Bai [28, 29]. Therefore, it can improve the separation efficiency of photogenerated carriers and supress the recombination of electron–hole pairs through the Z-scheme structure. In addition, the SPR of silver leads to the strong absorption to the visible light. The excellent conductivity of silver nanoparticles can enhance the electron translation so as to enhance the interfacial charge transfer efficiently, thus, the activity of Ag/AgI/AgBr/SPs photocatalyst is promoted exceedingly.

4 Conclusions

In summary, we develop a simple and facile ion exchange reaction along with photoreduction for the synthesis of the Z-scheme Ag/AgI/AgBr/SPs photocatalysts. Furthermore, Ag/AgI/AgBr/SPs photocatalysts exhibit excellent activity and stability compared with Ag/AgI and Ag/AgBr under visible light irradiation due to the synergistic effects between the Z-scheme structure of Ag/AgI/AgBr/SPs photocatalysts and the SPR effect of Ag NPs. Therefore, the as-prepared Ag/AgI/AgBr/SPs photocatalysts have potential application on pollutant degradation under sunlight.

Acknowledgements This work was supported by the National Natural Science Foundation of China (51404097, 51504083), Program for Science & Technology Innovation Talents in Universities of Henan Province (17HASTIT029), China Postdoctoral Science Foundation funded project (2016M592290) and Foundation for Distinguished Young Scientists of Henan Polytechnic University (J2016-2).

References

1. J.S. Xie et al., Mater. Lett. **120**, 54 (2014)
2. J. He et al., Appl. Catal. B **203**, 917 (2017)
3. C. Wang, C. Xu, H. Zeng, S. Sun, Adv. Mater. **21**, 3045 (2009)
4. Y.W. Jun, J.S. Choi, J. Cheon, Chem. Commun. **12**, 1203 (2007)
5. C. Wang, W. Tian, Y. Ding, Y.Q. Ma, Z.L. Wang, N.M. Markovic, V.R. Stamenkovic, H. Daimon, S. Sun, J. Am. Chem. Soc. **132**, 6524 (2010)
6. C.H. Cui, H.H. Li, J.W. Yu, M.R. Gao, S.H. Yu, Angew. Chem. **122**, 9335 (2010)
7. L.S. Zhang, K.H. Wong, Z.G. Chen, J.C. Yu, J.C. Zhao, C. Hu, C.Y. Chan, P.K. Wong, Appl. Catal. A **363**, 221 (2009)
8. L.S. Zhang, K.H. Wong, H.Y. Yi, C. Hu, J.C. Yu, C.Y. Chan, P.K. Wong, Environ. Sci. Technol. **44**, 1392 (2010)
9. H. Tada, T. Mitsui, T. Kiyonaga, T. Akita, K. Tanaka, Nat. Mater. **5**, 782 (2006)
10. S.H. Shen, L.J. Guo, X.B. Chen, F. Ren, C.X. Kronawitter, S.S. Mao, Int. J. Gre. Nanotechnol. **1**, M94 (2010)
11. H.M. Zhu, B.F. Yang, J. Xu, Z.P. Fu, M.W. Wen, T. Guo, S.Q. Fu, J. Zuo, S.Y. Zhang, Appl. Catal. B **90**, 463 (2009)
12. Z.F. Liu, Z.G. Zhao, M. Miyauchi, J. Phys. Chem. C **113**, 17132 (2009)
13. Z.F. Liu, M. Miyauchi, Chem. Commun. **15**, 2002 (2009)
14. X.F. Wang, S.F. Li, Y.Q. Ma, H.G. Yu, J.G. Yu, J. Phys. Chem. C **115**, 14648 (2011)
15. Y. Sasaki, A. Iwase, H. Kato, A. Kudo, J. Catal. **259**, 133 (2008)
16. Y. Sasaki, H. Nemoto, K. Saito, A. Kudo, J. Phys. Chem. C **113**, 17536 (2009)
17. K. Maeda, M. Higashi, D.L. Lu, R. Abe, K. Domen, J. Am. Chem. Soc. **132**, 5858 (2010)
18. M. Naderi, J.A. Dale, G.M.B. Parkes et al., React. Funct. Polym. **1**, 25 (2002)
19. C.A. Toro, R. Rodrigo, J. Cuellar, React. Funct. Polym. **9**, 1325 (2008)
20. F.M.B. Coutinho, R.R. Souza, A.S. Gomes, Eur. Polym. J **7**, 1525 (2004)
21. H.G. Yu et al., Appl. Catal. B **144**, 75 (2014)
22. H.G. Yu et al., Appl. Catal. B **187**, 163 (2016)
23. H. Tang et al., Appl. Surf. Sci **391**, 440 (2017)
24. M. Ahmed et al., Eur. Polym. J. **8**, 1609 (2004)
25. A.L. Linsebigler, G. Lu, J.T. Yates, Chem. Rev. **3**, 735 (1995)
26. X. Zhang, L.Z. Zhang, T.F. Xie, D.J. Wang, J. Phys. Chem. C **113**, 7371 (2009)
27. L. Ye, J. Liu, C. Gong et al., ACS Catal. **2**, 1677 (2012)
28. Y.Y. Bai, F.R. Wang, J.K. Liu, Ind. Eng. Chem. Res. **37**, 9873 (2016)
29. Y.Y. Bai, Y. Lu, J.K. Liu, J. Hazard. Mater. **307**, 26 (2016)